Activating Mutations in TOR Are in Similar Structures As Oncogenic Mutations in PI3KCα

Thomas W. Sturgill*,† and Michael N. Hall‡

†Department of Pharmacology, University of Virginia Health Sciences Center, Charlottesville, Virginia 22908 and
‡Biozentrum, University of Basel, CH-4056 Basel Switzerland

Discovery programs for cancer therapy are intently in pursuit of drugs to inhibit the class I phosphoinositide-3-OH-kinase (PI3K) and target of rapamycin (TOR) protein kinase (*1*). PI3K and TOR activate PKB (also known as Akt) in response to growth factors (*2, 3*). PI3K induces PDK1 to phosphorylate the activation loop of PKB (Thr308). TOR, in TOR complex 2, phosphorylates Ser473 in the C-terminal hydrophobic motif of PKB (*3*). Active PKB in turn switches on growth and survival pathways (*1*). TOR complex 1, activated in response to growth factors and nutrients, also contributes to cell growth by phosphorylating the translation regulators S6K and 4E-BP. Genetic abnormalities in cancers frequently result in activation of PKB, by loss of the tumor suppressor PTEN or by activating mutations of PI3KCα. Other class I PI3KCs are also deregulated in cancer, depending on the malignancy (*1*). A current goal is to bring compounds that inhibit specific PI3KC subtypes to clinical trials as soon as possible. Structures for PI3KCα (*4*) and PI3KCγ (*5–7*) have greatly aided drug design for PI3K and have provided insight on the enzymatic function and regulation of PI3K. (For abbreviations and acronyms used, see ref 8.)

Class I PI3Ks are bound and activated by Ras-GTP. Ras-GTP binding leads to derepression of inter- or intramolecular steric inhibition and targeting of PI3K to membranes by adapters (*9*). All class I PI3K enzymes have several domains in common, including a RBD (Ras-binding domain), a C2-domain, a helical domain, and a catalytic domain. PI3Ks are well-understood in comparison to PI3K-related protein kinases such as TOR, due in part to the availability of structures for PI3K, including a structure for a Ras-activated form of PI3KCγ (*10*).

The PI3K-related kinases (PIKKs), including TOR, Mec1/ATR, Tel1/ATM, SMG-1, and DNA-PK (see ref 11 for overview) have a catalytic domain related to PI3K but

ABSTRACT TOR (Target of Rapamycin) is a highly conserved Ser/Thr kinase and a central controller of cell growth. Using the crystal structure of the related lipid kinase PI3KCγ, we built a model of the catalytic region of TOR, from the FAT domain to near the end of the FATC domain. The model reveals that activating mutations in TOR, identified in yeast in a genetic selection for Rheb-independence, correspond to hotspots for oncogenic mutations in PI3KCα. The activating mutations are in the catalytic domain (helices kα3, kα9, kα11) and the helical domain of TOR. Docking studies with small molecule inhibitors (PP242, NVP-BEZ235, and Ku-0063794) show that drugs currently in development utilize a novel pharmacophore space to achieve specificity. Thus, our model provides insight on the regulation of TOR and may be useful in the design of new anticancer drugs.

*Corresponding author,
tws7w@virginia.edu.

```
                 1880      1890      1900      1910      1920      1930      1940      1950      1960      1970
TOR     1878 LMYTVPAVQGFFRSISLSRGNNLQDTLRVLTLWFDYGHWPDVNEALVEGVKAIQIDTWLQVIPQLIARIDTPRPLVGRLIHQLLTDIGRYHPQALIYPLT
TOR2Sc  1818 HRHVIPAIKGFFHSISLSESSSLQDALRLLTLWFTFGGIPEATQAMHEGFNLIQIGTWLEVLPQLISRIHQPNQIVSRSLLSLLSDLGKAHPQALVYPLM
TOR1Sc  1815 QRHVVPAIKGFFHSISLLETSCLQDTLRLLTLLFNFGGIKEVSQAMYEGFNLMKIENWLEVLPQLISRIHQPDPTVSNSLLSLLSDLGKAHPQALVYPLT
TOR2Sp  1681 EQYIIPAVKGFFKSIALSKGN-LQDTLRLLNLWFKFGNNSNVINTLNVGISTVNIDIWLDVIPQLIARIHASSLSVRKSVHQLLSDVGRAHPQALVYPLT
PI3Kα    495 HANWSVSREAGFSYSHAGLSNRLARDNELRENDKEQLKAISTRDPLSEITEQEKDFLWSHRHYCVTIPEILPKLLLSVKWNSRDEVAQMYCLVK-----D
PI3Kγ    519 LLDNYCHPIALPKHRPTPDPEGDRVRAEMPNQLRKQLEAIIATDPLNPLTAEDKELLWHFRYESLKDPKAYPKLFSSVKWGQQEIVAKTYQLLAKREVWD
                                              hA1              hB1    hB1'    hA2          hB2      hB2'
1e8X

                 1980      1990      2000      2010      2020      2030      2040      2050      2060      2070
TOR     1978 VASKSTTTARHNAANKILKNMCEHSNTLVQQAMMVSEELIRVAILWHEMWHEGLEEASRLYFGERNVKGMFEVLEPLHAMMERGPQTLKETSFNQAYGRD
TOR2Sc  1918 VAIKSESLSRQKAALSIIEKMRIHSPVLVDQAELVSHELIRMAVLWHEQWYEGLDDASRQFFGEHNTEKMFAALEPLYEMLKRGPETLREISFQNSFGRD
TOR1Sc  1915 VAIKSESVSRQKAALSIIEKIRIHSPVLVDQAELVSHELIRVAVLWHELWYEGLDEASRQFFVEHNIEKMFSTLEPLHKHLGNEPQTLSEVSFQKSFGRD
TOR2Sp  1780 VAAKSQSSARQNAALAIMDSLKTHSPRLVEQARLVSHELIRAAILWHEQWHEGLEEASRLYFGDHNIEGMFAVLEPLHEMLERGPETLREISFQQAFGRD
PI3Kα    590 WPPIKPEQAMELLDCNYPDPMVRGFAVRCLEKYLTDDKLSQYLIQLVQVLKYEQYLDNLLVRFLLKKALTNQRIGHFFFWHLKSEM-HNKTVSQRFGLLL
PI3Kγ    619 QSALDVGLTMQLLDCNFSDENVRAIAVQKLES-LEDDDVLHYLLQLVQAVKFEPYHDSALARFLLKRGLRNKRIGHFLFWFLRSEIAQSRHYQQRFAVIL
              hA3          hB3           hA4              hB4          hA5              hB5
1e8X

                 2080      2090      2100      2110      2120      2130      2140      2150      2160      2170
TOR     2078 LMEAQEWCRKYMKSGNVKDLTQAWDLYYHVFRRISKQLPQLTSLELQYVSPKLLMCRDLELAVPGTYD-PNQPIIRIQSIAP-SLQVITSKQRPRKLTLM
TOR2Sc  2018 LNDAYEWLMNYKKSKDVSNLNQAWDIYYNVFRKIGKQLPQLQTLELQHVSPKLLSAHDLELAVPGTRASGGKPIVKISKFEP-VFSVISSKQRPRKFCIK
TOR1Sc  2015 LNDAYEWLNNYKKSKDINNLNQAWDIYYNVFRKITRQIPQLQTLDLQHVSPQLLATHDLELAVPGTY-FPGKPTIRIAKFEP-LFSVISSKQRPRKFSIK
TOR2Sp  1880 LVEARDCCIRFEQTGDISDLNQADLYYQVFKKIRKQLPQLTTLDLQYVSPKLLHVHDLELAVPGTY-VSGKPVIRIVKFYP-TFNVITSKQRPRLSIK
PI3Kα    689 ESYCRACGMYLKH-LNRQVEAMEKLINLTDILK---QEKKDETQKVQMKFLVEQMRRPDFMDALQGFLSPLNPAHQLGNLRLKECRIMSSAKRPLWLNWE
PI3Kγ    718 EAYLRGCGTAMLHDFTQQVQVIDMLQKVTIDIKSLSAEKYDVSSQVISQL-KQKLENLQNLNLPQSFRVPYDPGLKAGALVIEKCKVMASKKKPLWLEFK
                 kα1              kα2              kβ1      kβ2      kβ3      kβ4
1e8X

                 2180      2190      2200      2210      2220      2230      2240      2250      2260
TOR     2176 GSNG------HEFVFLLKGHEDLRQDERVMQLFGLVNTLLANDPTSLRKNLSIQRYAVIPLSTNSGLIGWVPHCDTLHALIRDYREKKKILLNIEHRIML
TOR2Sc  2117 GSDG------KDYKYVLKGHEDIRQDSLVMQLFGLVNTLLQNDAECFRRHLDIQQYPAIPLSPKSGLLGWVPNSDTFHVLIREHREAKKIPLNIEHWVML
TOR1Sc  2113 GSDG------KDYKYVLKGHEDIRQDSLVMQLFGLVNTLLKNDSECFKRHLDIQQYPAIPLSPKSGLLGWVPNSDTFHVLIREHRDAKKIPLNIEHWVML
TOR2Sp  1978 GSDG------KDYQYVLKGHEDIRQDERVMQLFGLCNNLLLADPETFKRLLSIQRYPVIPLSPDSGLLGWVLDSDTLHVLIRDYRESRKILLNIEHRLII
PI3Kα    785 NPDIMSELLFQNNEIIFKNGDDLRQDMLTLQIIRIMENIWQNQG----LDLRMLPYGCLSIGDCVGLIEVVRNSHTIMQIQCKGGLKGAL----------
PI3Kγ    817 CADPTALSN-ETIGIIFKHGDDLRQDMLILQILRIMESIWETES----LDLCLLPYGCISTGDKIGMIEIVKDATTIAKIQQSTVGNTGA----------
                 kβ5             kα3                kβ6      kβ7      kβ8 kα4
1e8X

                 2270      2280      2290      2300      2310      2320      2330      2340      2350      2360
TOR     2270 RMAPDYDHLTLMQKVEVFEHAVNNTAGDDLAKLLWLKSPSS--EVWFDRRTNYTRSLAVMSMVGYILGLGDRHPSNLMLDRLSGKILHIDFGDCFEVAMT
TOR2Sc  2211 QMAPDYDNLTLLQKVEVFTYALNNTEGQDLYKVLWLKSRSS--ETWLERRTTYTRSLAVMSMTGYILGLGDRHPSNLMLDRITGKVIHIDFGDCFEAAIL
TOR1Sc  2207 QMAPDYENLTLLQKIEVFTYALDNTKGQDLYKILWLKSRSS--ETWLERRTTYTRSLAVMSMTGYILGLGDRHPSNLMLDRITGKVIHIDFGDCFEAAIL
TOR2Sp  2072 QMAPDYDRLTLLQKVEVFEYALLSTTGQDLYRVLWLKSRSS--EAWLNRRTNYSRTLAVMSMVGYILGLGDRHPSNLMLDRYTGNIIHIDFGDCFEVAMH
PI3Kα    871 -----------------------QFNSHTLHQWLKDKNKG-EIYDAAIDLFTRSCAGYCVATFILGIGDRHNSNIMVKD-DGQLFHIDFGHFLDHKKK
PI3Kγ    902 -----------------------FKDEVLSHWLKEKCPIEEKFQAAVERFVYSCAGYCVATFVLGIGDRHNDNIMISE-TGNLFHIDFGHILGNYKS
                              kα5            kα6                      kβ9      kβ10
1e8X

                 2370      2380      2390      2400      2410      2420      2430      2440      2450
TOR     2368 REKFP-EKIPFRLTRMLTNAMEVTG-------LDGNYRITCHTVMEVLREHKDSVMAVLEAFVYDPLLNWRLMDTNTKGNKRSRTRTDSYSAGQSVEIL
TOR2Sc  2309 REKFP-EKVPFRLTRMLTYAMEVSG-------IEGSFRITCENVMKVLRDNKGSLMAILEAFAFDPLINWGFDLP----------------TKKIEEET
TOR1Sc  2305 REKYP-EKVPFRLTRMLTYAMEVSG-------IEGSFRITCENVMRVLRDNKESLMAILEAFALDPLIHWGFDLP----------------PQKLTEQT
TOR2Sp  2170 REKFP-EKIPFRLTRMLVNAMEVSG-------IEGTFRITCEHVMRVLRTNKESVMAVLEAFVYDPLINWRLAPA--------------YSPSIDEKQS
PI3Kα    944 KFGYKRERVPFVLTQDFLIVISKG-AQECTKTREFERFQEMCYKAYLAIRQHANLFINLFSMMLGSGMPE-------------------------------
PI3Kγ    975 FLGINKERVPFVLTPDFLFVMGTSGKKTS---LHFQKFQDVCVKAYLALRHHTNLLIILFSMMLMTGMPQ-------------------------------
                 kα7            kα8            kα9
1e8X

                 2460      2470      2480      2490      2500      2510      2520      2530      2540
TOR     2459 DGVELGEPAHKKTGTTVPESIHSFIGDGLVKPEALNKKAIQIINRVRDKLTGRDFSHDDTLDVPTQVELLIKQATSHENLCQCYIGWCPFW
TOR2Sc  2384 GIQLPVMNANELLSNGAITEEEVQRVENEHKNAIRNARAMLVLKRITDKLTGNDIRRFNDLDVPEQVDKLIQQATSVENLCQHYIGWCPFW
TOR1Sc  2380 GIPLPLINPSELLRKGAITVEEAANMEAEQQNETKNARAMLVLKRITDKLTGNDIKRFNELDVPEQVDKLIQQATSIERLCQHYIGWCPFW
TOR2Sp  2247 NEPNTLLGETIDGLHRKRLNEEGITLEERQKPEILNQRAITVLNRVSNKLTGRDFKPQQQLDVPSQVEKLILQATSIENLCLCYIGWCSFW
PI3Kα   1013 -----------------LQSFDDIAYIRKTLALDKTEQEALEYFMKQMNDAHHGGWTTKMDWIFHTIKQHALN
PI3Kγ   1042 -----------------LTSKEDIEYIRDALTVGKSEEDAKKYFLDQIEVCRDKGWTVQFNWFLHLVLGIKQGEKHSA
                 kα10            kα11            kα12
1e8X
```
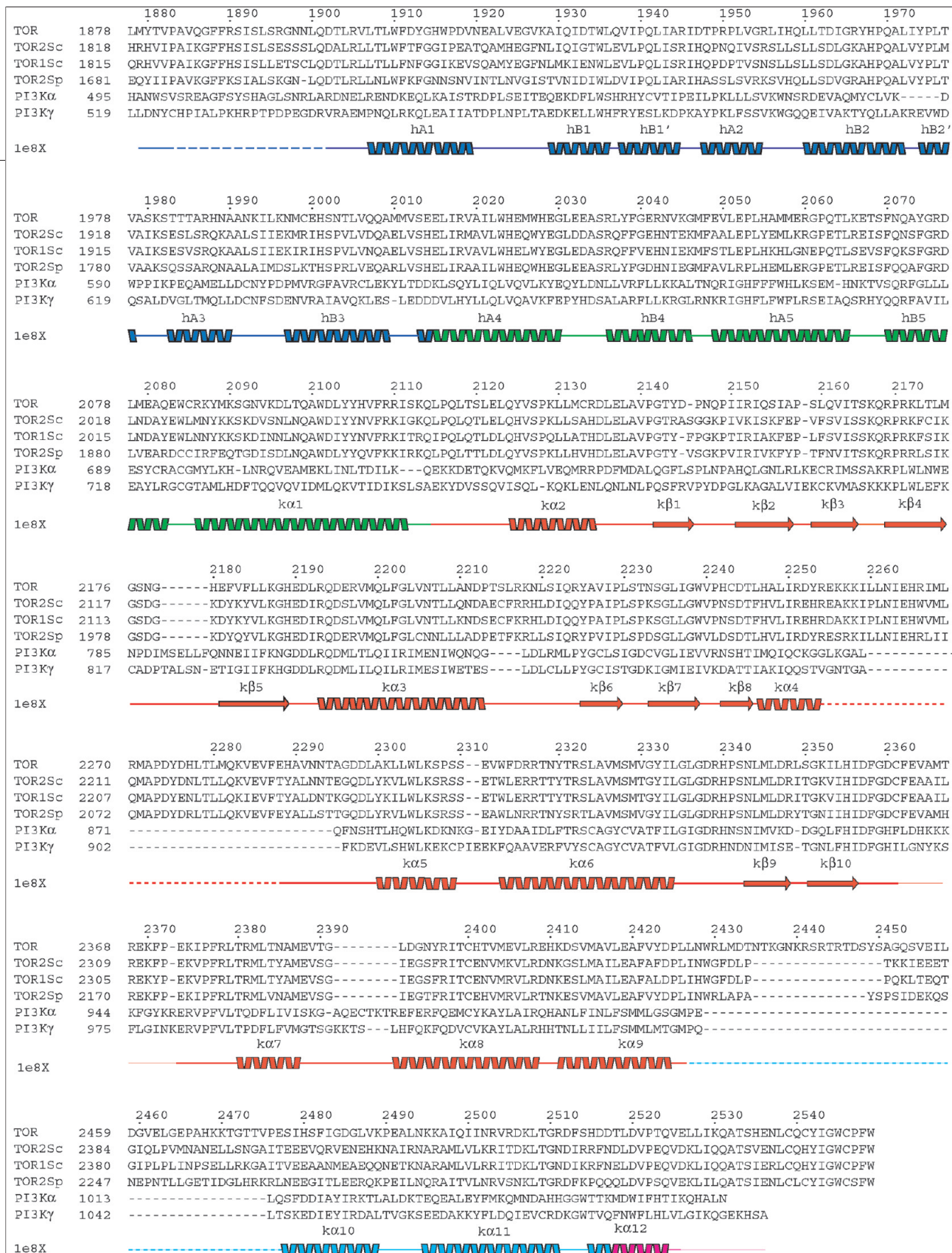
Figure 1. Structural alignment of TORs and PI3KC. The TORs are human TOR (NP_004949.1), *S. cerevisiae* TOR1 (P35169.3) (TOR1Sc) and TOR2 (P32600.3) (TOR2Sc), and *S. pombe* TOR2 (NP_595359.2) (TOR2Sp). The PI3KCs are human PI3KCα (CAA82333.1) and pig PI3KCγ (NP_999104.1). The structural elements are drawn from 1e8x and color-coded according to a scheme used throughout for TOR domains (8): FAT, sky blue; FRB, green, CAT, red; FIT (see text for domain definition), cyan; portion of the FATC, magenta. See Methods for tools used in this manual alignment.

are atypical Ser/Thr protein kinases. PIKKs control adaptive, checkpoint responses to genotoxic or nutritional stress activated in cancers. All are important drug targets, yet there is no structure available for the catalytic region of any PIKK. TOR signaling is particularly complex, as TOR is in two structurally and functionally distinct multiprotein complexes (TORC1 and TORC2) (2). TORC1 in all eukaryotes controls cell growth in response to nutrients (2, 3, 12). In metazoans, TORC1 also controls growth in response to growth factors. The growth factor signal, including insulin, is transmitted to TORC1 via PKB-mediated phosphorylation and inhibition of TSC1-TSC2, a heterodimeric GTPase activating protein (GAP) for Rheb. Upon inhibition of TSC1-TSC2, active Rheb binds and activates TORC1. The mechanism by which TORC1 integrates nutrient and growth factor signals is not clear but appears to occur at the level of TORC1. Growth factors also activate TORC2, but by an unknown mechanism independent of Rheb.

The PIKKs share a helical domain (FAT) of ~500 residues, a catalytic domain with motifs related to PI3K, and a short but highly conserved C-terminal FATC domain. The helical and FATC domains flank the catalytic domain. A portion of the helical domain in TOR is known as the FKB12-rapamycin binding (FRB) domain. Rapamycin inhibits TORC1 function by binding this domain. Rapamycin analogues are now approved anticancer drugs. However, variability in growth inhibition limits the potential of rapamycin analogues as single agents. Rapamycin analogues as single agents may not be effective anticancer agents because they do not inhibit TORC2 and because they inactivate a TORC1-mediated negative feedback loop, thereby increasing PKB and MAP kinase activity (2, 3, 13).

Recently, both academic and industry scientists have reported isolation of TOR inhibitors identified by activity screens (14–17). Some PI3K-inhibitors (PI-103 (14), NVP-BEZ235 (16)) selectively inhibit both PI3KC and TOR without appreciably inhibiting other protein kinases, including other PIKKs. Torin1 (17), PP242 (18), and Ku-0063794 (15) are more specific for TOR, whether TOR is in TORC1 or TORC2. Drug discovery urgently needs structures for PIKKs, and hopefully these are soon forthcoming. Attempts to model TOR to related PI3Ks, either for insights in drug design or for insights on regulation and function of TOR, have been hampered by the fact that the regions of obvious sequence similarity between TOR and PI3Ks are too limited for auto-

TABLE 1. Residues near to ATP in human TOR

Residue	In structure	Conservation[a]
Ser2165	$k\beta3-k\beta4$	100%, as Ser/Thr
Pro2169	$k\beta4$	100%
Lys2187	$k\beta5$	100%
Tyr2225	$k\beta6$	100%, as Tyr/Phe
Ile2237	$k\beta7$	100%, as Φ[b]
Val2240	$k\beta7-k\beta8$	98%, as Val
Met2345	$k\beta9$	81%[c]
Leu2354	$k\beta10$	100% as Φ[b]
Ile2356	$k\beta10$	96%[d]

[a]Percentages from one hundred and ten sequences. [b]Φ (Leu/Val/Ile/Met). [c]Leu 19% . [d]Val 4%.

mated alignment programs used by computational biologists. A homology-based model of part of the ATP-binding site of TOR was recently described (see Discussion).

We were able to build a model of the catalytic region of TOR based on the known crystal structure of PI3Kγ, after manual alignment of amino acid sequences of the two kinases. We identified new motifs, conserved between TORs and PI3Ks and also conserved between TOR and other PI3K-related kinases. Of particular interest, activating mutations in TOR structurally correspond to activating mutations in PI3KCα, suggesting a key regulatory role for the RQD (kα3) and kα9 helices in TOR. Furthermore, our model may be valuable for drug discovery, as shown by docking PP242, NVP-BEZ235, and Ku-0063794 into the active site and definition of putative binding modes in TOR.

RESULTS

Criteria for Alignment of TOR and PI3KC Sequences.
To construct a model of the structure of the TOR catalytic region, we aligned the sequences of TOR and PI3KC. To determine the catalytic region of TOR, we first compared ~100 TOR sequences from various organisms, by using ClustalW. We found blocks of conservation suggesting that the catalytic region of TOR begins near residue 1800 near the defined FAT domain. We then manually aligned amino acid sequences of several TORs and PI3KCs, beginning near the FAT and the helical domains, respectively, using several criteria and tools (see Meth-
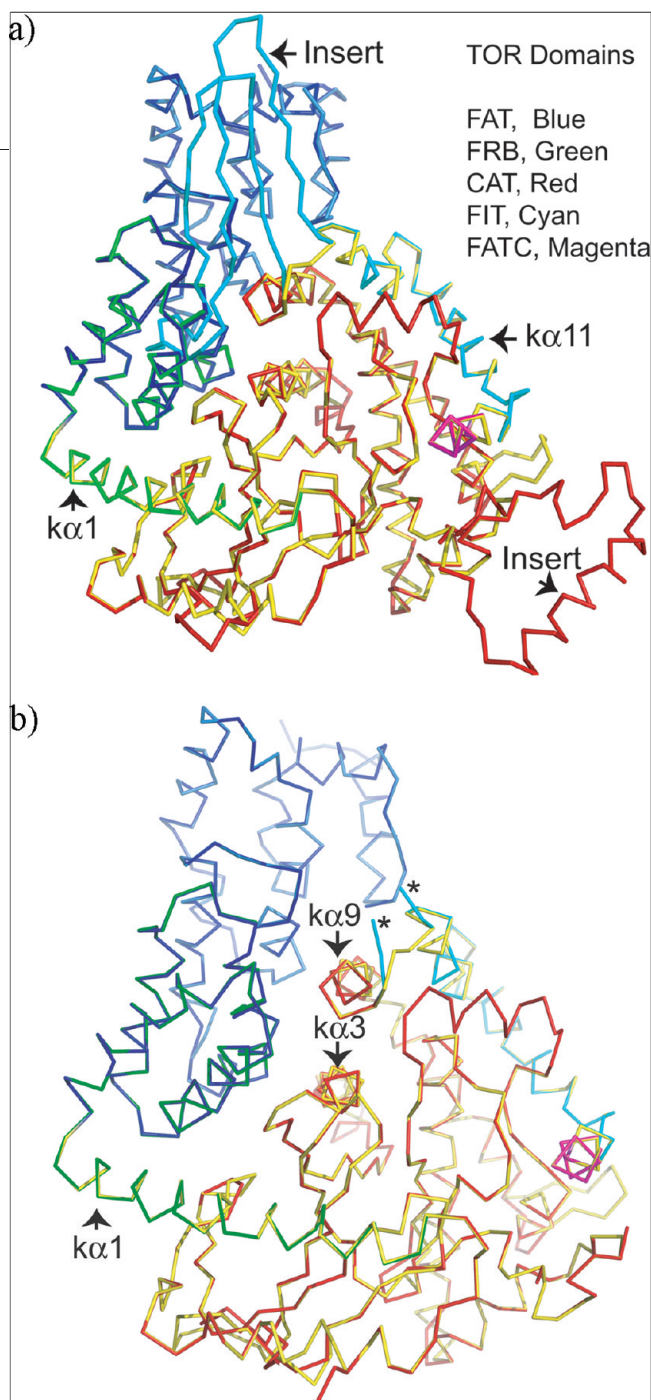
Figure 2. TOR compared to PI3KCγ. a) A portion of the FRB domain (**8**) corresponds to the helical domain (FAT (**8**) domain), and a portion is the helix kα1 of the catalytic domain of PI3KCγ. Two inserts cannot be modeled to PI3KCγ. One is early in the FIT (**8**) domain (defined as residues 2427−2516) between the catalytic and FATC domains. The other is in the catalytic domain. Coloring of PI3KCγ (1e8x): blue, helical domain; yellow, catalytic domain. The C-terminal part of the FIT domain forms the C-terminal helices in PI3KCγ (kα10-kα12). A portion of the FATC (**8**) has no template in 1e8x but either overlaps or is appended to kα12. **b)** A rotation shows the key structural roles of the RQD helix (kα3) and kα9. The kα9 ends the conserved catalytic domain of TOR. Insertion of the undefined portion of FIT domain is at the two stubs (asterisks).

ods). Our results are summarized in a structural alignment of five TORs and two PI3KCs (Figure 1). We looked for conserved residues in TORs taken from all across the animal and plant kingdoms (manuscript in preparation). We collected, validated, and trimmed ∼100 TORs so as to begin near residue 1860. Smaller sets of diverse sequences for PI3Ks (classes I, II, and III) were also collected and trimmed to begin at the helical domain. We evaluated many factors as we made the alignment, including conservations within homologous proteins, predictions of propensity of TOR residues for structure in different views in MacVector, as well as views of the PI3K structures at the NCBI with Cn3D. Hereafter, we use the defined structural elements from PI3KCγ (**6**) throughout for discussion. Furthermore, residue numbers given below for TOR refer to the position of the residues in human TOR, unless otherwise indicated.

Alignment of the Catalytic Loop of TOR. TORs have short regions of near identity that are the main features defining the PI3K-related kinase group. The segment 2180−2381 of human TOR is clearly similar to PI3KCγ. The motif K^{2187}GHEDL<u>RQD</u> is in the N-terminal lobe of the catalytic domain in TOR. In PI3KCγ, Lys2187 corresponds to the wortmannin-reactive lysine within the N-terminal lobe (in kβ5) and the conserved RQD (underlined) is in kα3 (**6**). There are other key motifs in residues 2260−2317 of TOR that contain strong identities to PI3KC. Ser2323 of TOR is in the center of a predicted helix equivalent to kα6 of PI3KCγ. This predicted helix is followed by the catalytic loop GLG<u>DRH</u>PS. The triplet DRH is always followed by a proline in TORs and defines a unique feature. Proline is never found at this position in any non-TOR PI3K-related kinase or in any PI3KCs or PI4K. The aspartate of the DRH motif (D2338 in TOR) is thought to be the catalytic base for the phosphate transfer reaction in protein kinases.

Alignment of the Activation Loop of TOR. The activation loop of TOR begins with a DFG motif. The aspartate of the DFG motif (D2357) positions a key Mg^{2+} ion necessary for catalysis. The end of the activation loop in TOR is less easily recognized. The end of the activation loop is usually defined by an APE motif in protein kinases. The activation loop of TOR has a conserved PE motif (residues 2372 and 2373). PE is conserved in this position in all of the PIKKs, but is absent in the activation loop of PI3Ks. The activation loop of PIKKs, as defined by the DFG and PE motifs, is considerably shorter than

the activation loop of protein kinases (14−15 residues versus 23−35 residues).

The activation loop of TOR ends with kα7. Part of kα7 is similar in sequence to the F-helix that follows the activation loop in the C-subunit of cyclic AMP-dependent protein kinase. A consensus for a sequence at the end of the activation loop in TOR, spanning the PE as well as a putative P+1 loop, can be given as PE (K/R) (V/I) PFRL. This motif is conserved in all TORs.

Alignment of ATP Binding Residues in TOR. ATP binds to PI3KCγ using polar contacts made to phosphates and hydrophobic contacts made to adenine (6). Building the ATP binding site requires short β-strands (kβ1−10 in PI3KCγ) which present conserved residues that contact ATP. This is unlike the ATP binding mode of typical protein kinases (19), which use the conserved, ATP-binding motif GxGxxGxV (x, any amino acid), not found in PI3KCs and PI3K-related kinases. Furthermore, the novel mode of ATP binding by PI3KCs requires a key serine (Ser806 in PI3KCγ) that interacts with the β-phosphate of ATP (6). We expected this mode of ATP binding in PI3KCγ to be conserved in TOR, and we sought to identify β-strands conserved in all TORs that correspond to kβ1−10 in PI3KCγ. Automated alignments have failed to align the region N-terminal to the equivalent of Ser806 critical for ATP binding. Predicted catalytic domains for TOR, such as CD05169 at NCBI, are unlikely to bind ATP because they commence too far toward the C-terminus, at best at Ile2153 in the middle of the equivalent of kβ2 in PI3KCγ. One factor contributing to this confusion may be that all of the PI3KCs (classes I−III) have a PxxP motif between kβ1 and kβ2, exactly 16 residues N-terminal to the serine equivalent to Ser806 in PI3KCγ, and this motif is not present in TOR or any other PI3K-related kinases. Thus, a key to making a structural alignment of TOR to PI3KCγ for homology modeling was to discover the conserved residues presented by kβ1−10 in TOR. The residues we identified are summarized, with their conservation in the ~100 TOR sequences, in Table 1. Identification of these residues locates kβ3−10 in TOR. We then identified the probable boundaries of the β-strands based on conservations and propensity to form β-strands using tools in MacVector during manual alignment. We then adjusted gaps between the predicted kβ1−5 in this region (Figure 1).

Ser2165 in TOR corresponds to Ser806 in PI3KCγ, presented in the loop between kβ3 and kβ4 to interact with the β-phosphate of ATP. This serine is characteris-tic for a mode of ATP binding predicted to be shared by TOR and is 100% conserved in TORs. Ser2165 is aligned in automated alignments of PI3KCs to TORs. Further-more, the kβ1−4 strands were difficult to identify in TORs, but a key proline helped define a boundary for kβ1 in TORs. This proline, Pro2141, is conserved in 100% of TORs. Pro780 in PI3KCγ aligns with Pro2141 in TOR. Pro780 appears to be conserved in all PI3KCγ's from different species.

We identified other residues in TOR that should be near ATP, also summarized with their conservation in Table 1 and amplified upon as follows. Lys2187 in kβ5 has to be in the ATP pocket. This lysine (Lys833 in PI3KCγ) should interact with the α-phosphate of ATP. Pro2170 is conserved in all PIKKs and is equivalent to Pro810 in PI3KCγ. Pro810 packs against the hydrocar-bons of the side chain of Lys833, in a position to stabi-lize the interactions of the ε-amine of Lys833 for cataly-sis. Tyr2225 in kβ6 has to be positioned in a specific conformation if TOR is to bind ATP. Tyr2225 corresponds to Tyr867 in PI3KCγ. Tyr867 is positioned with the phe-nolic ring nearly perpendicular to the adenine ring of ATP and with adenine C6-NH2 4 Å away. This aromatic hy-drophobic residue is conserved as tyrosine or phenylala-nine in all PI3Ks and PIKKs. Ile2237 is in motif GLIGW in kβ7. Gly2235 begins a similar motif found in the cata-lytic domain of every PI3K and PIKK. The two residues af-ter Gly2235 are always hydrophobic. Ile2237 is Ile879 of P3KCγ. Ile2237 aligns with the so-called gatekeeper residues in other kinases. The hinge region (residues 2238−2246) adjacent to the gatekeeper contains Val2240, located between kβ7 and kβ8, that should make interactions with the adenine ring of ATP. This Val882 in PI3KCγ lies at the bottom of the ATP pocket. The short loop between kβ7 and kβ8 is the deepest wall of the ATP binding pocket (6), and Val882 provides two hydrophobic contacts with adenine. Met2345 is in kβ9, a β-strand in the predicted larger lobe of the kinase. Leu2354 precedes the DFG motif, replacing Phe961 in PI3KCγ. The aromatic ring of Phe961 is at the bottom of the ATP pocket. This phenylalanine is found in ~100% of PI3K sequences (classes I, II, III), and precedes the DFG motif of the activation loop. In all TORs, as well as in PI3K-related kinases in general, this residue is never aromatic and is always an aliphatic hydrophobic residue (Leu/Val/Ile/Met).

Identification of a WLK Motif in TOR. We identified an insertion that we place between kα4 and kα5 in
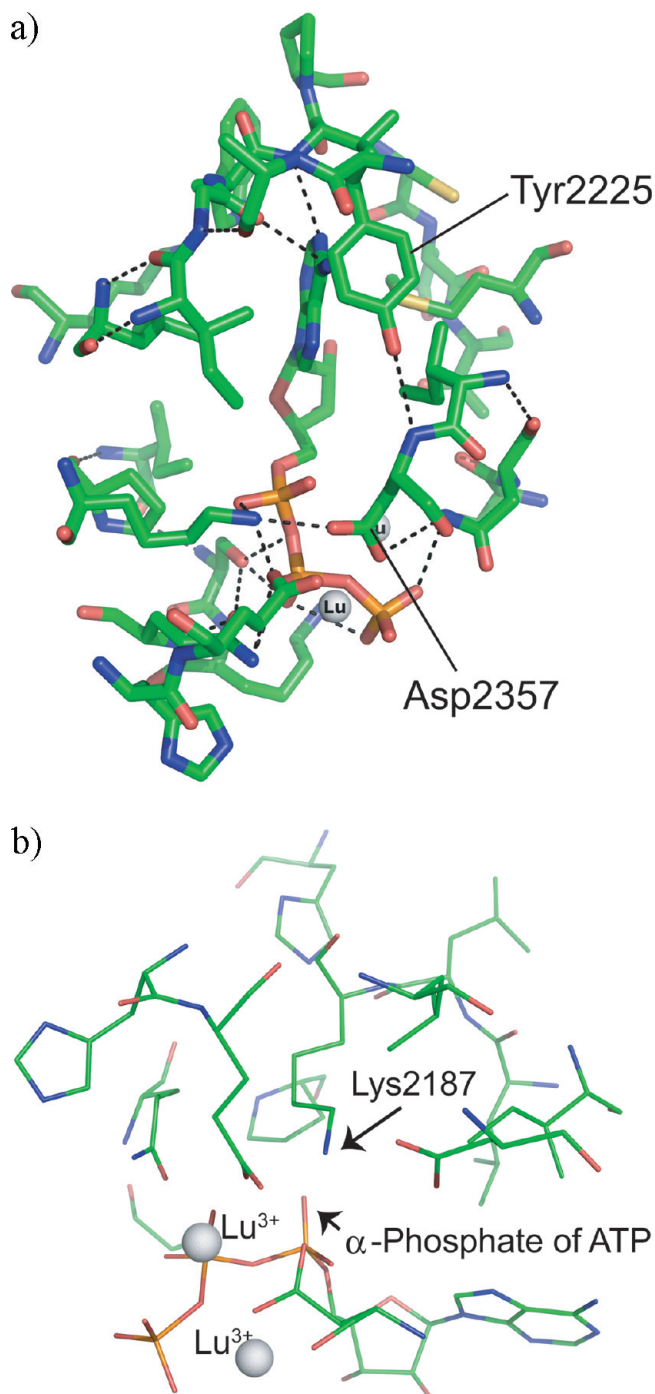
a)

b)

Figure 3. Residues binding ATP in TOR. a) Orientation of adenine N-6 to Tyr2225 in TOR. Asp2357 is near the γ- and β-phosphates of ATP. b) Lys2187 is near the α-phosphate of ATP.

TOR. Placement of the insertion (residues ∼2254−2288) was helped by discovery of a WLK motif that identifies kα5. The WLK sequence is in >90% of TORs. The tryptophan (Trp2304) is particularly well conserved, found in 100% of the approximately 100 TOR sequences examined. A similar motif is present in almost all PI3KCs (classes I and II). Recognition of the WLK motif as marking kα5 facilitated subsequent alignments. There is a shorter gap in TORs in the surface loop that lies between kα7 and kα8 in PI3KCγ. This is then followed by longer helices kα8 and kα9 that are similar to helices in PI3KCγ.

End of the Catalytic Domain. The end of conservation in the catalytic domain in TORs occurs abruptly, marked by an invariant FxxDPL motif (F[2421]xxDPL in human TOR). The next residue is also strongly conserved (97%) as isoleucine or leucine. We also found a nearly invariant arginine in TORs and other PI3K-related kinases near this motif, Arg2408 in human TOR. This is notable because a conserved arginine is very near the end of the catalytic domain of Ser/Thr kinases. The conserved arginine (Arg280 in PKA C-subunit) defines subdomain (XI) in the protein kinases. Arg1021 in human PI3KCγ is conserved in all class I PI3KCs that we have examined, and aligns with Arg2408 in human TOR. However, Arg1021 in porcine PI3KCγ is not playing the same structural role as Arg280. Arg280 in PKA makes a salt bridge to Glu208 in the APE motif at the end of the activation loop (19).

Alignment of Helical Domains. We placed predicted helices from the FAT domain and the defined helices from the FRB domain upon the defined helices in PI3KCγ. This region lacks sufficient similarity to be aligned by means other than superimposition of potentially corresponding helices, using tools in MacVector to view potential for helicity according to several scoring systems. The alignment of predicted helices can be improved by introduction of gaps, but we made the alignment that places predicted helices near defined helices in PI3KCγ assuming there were no gaps. The entire FRB domain (residues 2015−2114) is highly similar in the approximately 100 TORs examined. The FRB domain contains a few residues that are invariant in all the TORs, including Glu2015, Leu2016, Arg2017, Glu2025, and Trp2027 in the sequence ELIRVAILWHE. This key motif falls near hα4 in PI3KCγ.

Insertion of the FIT domain of TOR. We name the portion of the C-terminus of TOR from FxxDPL to the FATC do-

main (residues 2427−2516) the FIT domain (Found in TOR). FIT is a useful short acronym and a phonetic contrast to the FAT and FATC domains. The FIT domain shows more divergence in our ~100 TORs than the catalytic domain, but is highly conserved within specific taxonomic subgroups.

The FIT domain contains an insertion relative to PI3KCγ. We suggest that the insertion is at the position corresponding to the very short surface loop between kα9 and kα10 of PI3KCγ. This loop opens to a vacant space in the PI3KCγ structure above the active site in PI3KCγ, placing Ser2481 near the active site of TOR. In this context, it is important to note that there is considerable interest in the FIT domain as a regulatory domain because of three findings: (i) Ser2448 is phosphorylated by S6K1 (20), (ii) the ΔRD mutant deleting Ser2448 is more active as a kinase (21), and (iii) TOR autophosphorylates Ser2481 when TOR is present in TORC2 (22, 23).

Alignment of the FATC Domain. A helix is predicted to start in human TOR after Pro2522. The helix determined in the NMR structure (RCSB, PDB 1w1n) of the refolded FATC of *S. cerevisiae* TOR1 begins at Glu2444 following Pro2443 (equivalent to Pro2522 in human TOR) (24). Pro2522 in human TOR is conserved in all ~TORs. The next residue, Thr2523 in human TOR and Glu2444 in *S. cerevisiae* TOR1, is not conserved in the ~100 TORs. Strikingly, the second residue, Gln2524 in human and Gln2445 in *S. cerevisiae*, is conserved in the ~100 TORs. Other invariant residues (numbered by human) are Leu2528, Ala2532, Gly2544, and Trp2545. We chose an alignment that places the defined helix near, not upon, kα12 so as to minimize the size of the gap in PI3KCγ and to align predicted helices near the end of the FIT domain with kα10 and kα12.

Making a TOR Structure. We used computer routines provided in the SWISS-MODEL (8.05) server (25) to build a model for the catalytic region of TOR based on the above manual alignment of TOR and PI3KCγ (Figure 1). The template was PI3KCγ (RCSB, PDB 1e8x). This template is a structure for an inactive form of PI3KCγ with bound ATP (6). The modeled catalytic region of human TOR is residues 1906−2526.

The backbone structures of human TOR and PI3KCγ are compared in Figure 2. The TOR model shows that the FRB domain (residues 2015−2114) corresponds to a portion of both the helical domain and the catalytic domain of PI3KCγ. The FRB domain covers helices hA4,
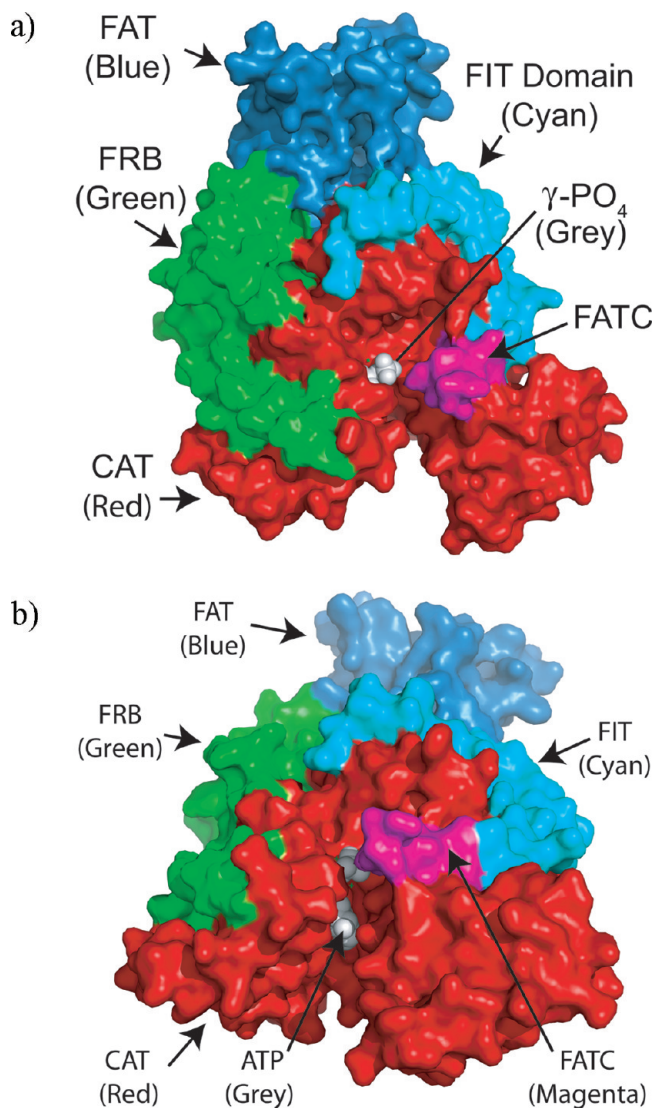
Figure 4. Pharmacophore space in TOR. a) The γ-phosphate of ATP (gray) is exposed. b) A pharmacophore space lies below the active site. This space is also in the PI3KCγ structure (see Supplementary Figure S1). See ref 8 for definitions of domain acronyms FAT, FRB, CAT, FIT, and FATC.

hB4, hA5, and hB5 of the helical domain and helix kα1 of the catalytic domain of PI3KCγ.

There is an insert in TOR in the catalytic domain (chain colored red) in the loop between kα4 and kα5 (Figure 2, panel a). This loop is ten residues in PI3KCγ, and is expanded to ~47 residues in TOR. The first residues (REKKK) of this loop in TOR form a cluster of charged residues that imposes a requirement for surface exposure.

Based on secondary structure predictions, the expanded loop between kα4 and kα5 may remain as a loop or form a surface helix−loop−helix.

The FIT domain (chain colored in cyan) is mostly undefined in the TOR model (Figure 2, panel a). Sequences toward the end of the FIT domain form helices kα10 and kα11. A portion (chain colored in magenta) of the FATC domain corresponds to kα12. Residues in the terminating helix kα12 (residues 1081−1090) and in the remainder of the C terminus (residues 1091−1102) of PI3KCγ are closer to ATP than generally appreciated. The side chain NH_2 of Gln1083 in kα12 of PI3KCγ is 10.6 Å from oxygen of the γ-phosphate. Trp1086 in kα12 is within 12 Å of the γ-phosphate. These distances are too large for direct contacts. However, no other residues lie between Gln1083 and Trp1086 and the γ-phosphate in the structure of ATP-bound PI3KCγ, suggesting that these residues either line a substrate pocket or sterically inhibit access of substrate. The portion of the FATC domain that was not modeled (residues 2527−2549) is short and, whatever its fold, is constrained to also be near the active site. Thus portions of the FATC domain

(RCSB, PDB 1w1n), including the helix and unique Cys-containing structure, which cannot be modeled, are likely to be close to the active site in a determined structure.

In Figure 2b, the undefined portions of TOR are trimmed to visible stubs, and the superimposed backbones for the TOR model and PI3KCγ are rotated so as to look along the axis of helix kα3. The stubs (cyan, asterisks) show where the undefined portion of the FIT domain is inserted in TOR. The FIT domain emerges above the active site, where there is space for a subdomain on the surface of the C-terminal lobe of the catalytic domain before its C-terminal portion merges into kα10 and kα11. The first and last residues of the FIT domain shown (cyan) are Asn2428 and Val2475. Ser2481, which is autophosphorylated by TOR in TORC2 (22), must be near the active site of TOR. Insertion of the FIT domain at the surface loop between helices kα10 and kα11 of PI3KCγ may place Ser2481 near the active site where it can be phosphorylated.

The kα3 and kα9 helices were built and superimposed upon the corresponding helices from PI3KCγ.

This fulfills a key criterion for modeling a correct catalytic domain for TOR. The kα3 and kα9 helices run through the core of PI3CKγ and above the active site. The helix kα3 (the RQD motif-containing helix) positions residues in the loop preceding RQD near the active site. In the view of Figure 2, panel b, kα3 runs into the page. After building the remaining β-sheet elements required for the ATP pocket, the polypeptide chain returns to the opposite side of the molecule to pass back through the core as helix kα9. The returning helix kα9 runs nearly parallel to kα3 and above it, but with an opposite directional vector. Thus, helix kα9, which comes in linear sequence from near the C-terminus, is placed in position to stabilize kα3. Correct placement of kα9 above kα3 in TOR required discovery of the gaps and inserts as shown in the structural alignment (Figure 1).

ATP Binding to TOR. Residues in TOR equivalent to residues for ATP binding in PI3KCγ (Table 1) are shown in relation to ATP and two Lu^{3+} ions from the 1e8x template (Figure 3). The plane of the adenine ring of ATP in TOR is nearly perpendicular to that of Tyr2225, with the C6-NH2 of the adenine ring pointing toward the aromatic ring of Tyr2225. The ε-NH2 of Lys2187 is 3.32 and 3.49 Å in distance from an oxygen of the α-phosphate of ATP (Figure 3, panel b). Ser2165 is in proper position with its side chain -OH pointing toward oxygens of the β-phosphate of ATP (not shown). This mode of ATP binding supports the structure built for TOR on the PI3KCγ template.

Surface views of ATP in TOR reveal an important finding (Figure 4). The domains of TOR are again colored as for the backbone structure of TOR. One sees an expected pocket in the catalytic domain (colored in red) that lies above and beside the γ-phosphate of ATP (colored in gray) (Figure 4, panel a). The missing portion of the FIT domain emerges somewhere above this pocket in our model. The surprise is that, in the TOR model, portions of the ribose ring are not buried but are exposed in a groove that extends along the bottom of the substrate pocket (Figure 4, panel b). Portions of the adenine ring of ATP are also visible (not shown). In structures of PKA, adenine and the ribose are completely buried, in the most closed structure with ATP and inhibitor peptide (1ATP) and in the structure for a transition state mimic (19). The observation we make here for TOR is also seen with a similar projection for PI3KCγ. ATP is partially exposed in a similar groove that is below the active site of PI3KCγ (Supplementary Figure S1).

a) *S. cerevisiae* TOR1

b)
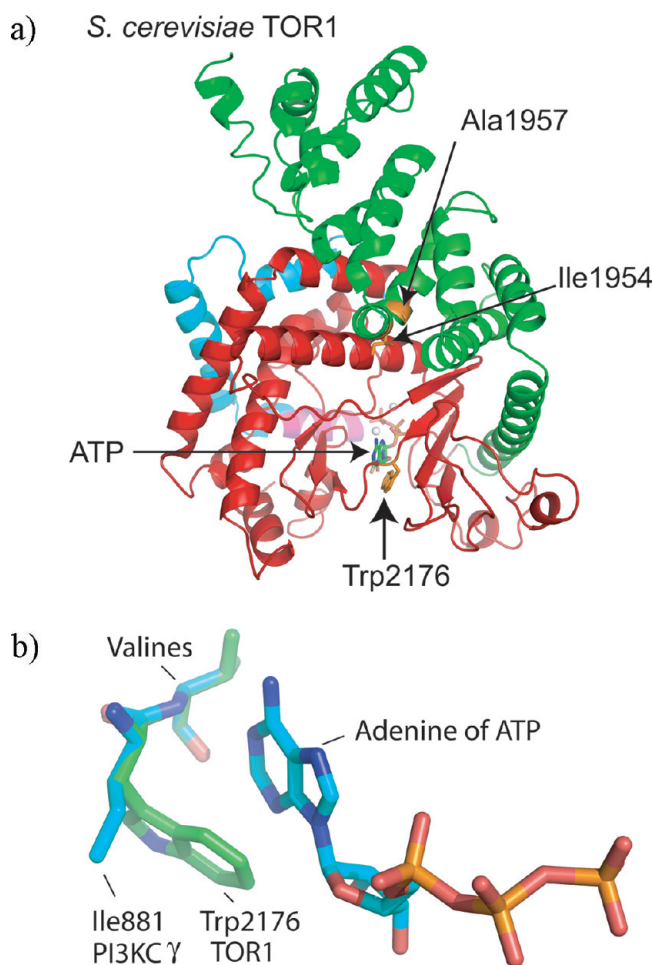
Figure 5. Location of mutations in model of *S. cerevisiae* TOR1. a) Mutation of Trp2176 in the adenine pocket increases resistance to caffeine. Mutations of Ile1954 and Ala1957 in the FRB domain activate TOR1. View is from the back. b) Trp2176 is a TOR-specific difference in the adenine pocket. Enlarge to see side chains (orange) of mutated residues.

Yeast TOR Protein Mutations. Characterized mutations in yeast TOR proteins (Table 2) can be used to validate our model. Caffeine is a TORC1 inhibitor, and a genetic selection for caffeine resistance in *S. cerevisiae* identified mutations in TOR1 (26). Caffeine, which mimics adenine, can bind a subset of sites for adenine nucleotides, including the site in the PI3K-related kinase ATM (27), but appears to be more specific for TORs in TORC1 *in vivo* in comparison to other PIKKs (28). The caffeine resistance mutations in TOR1 decrease affinity for caffeine or confer increased TORC1 kinase activity. The
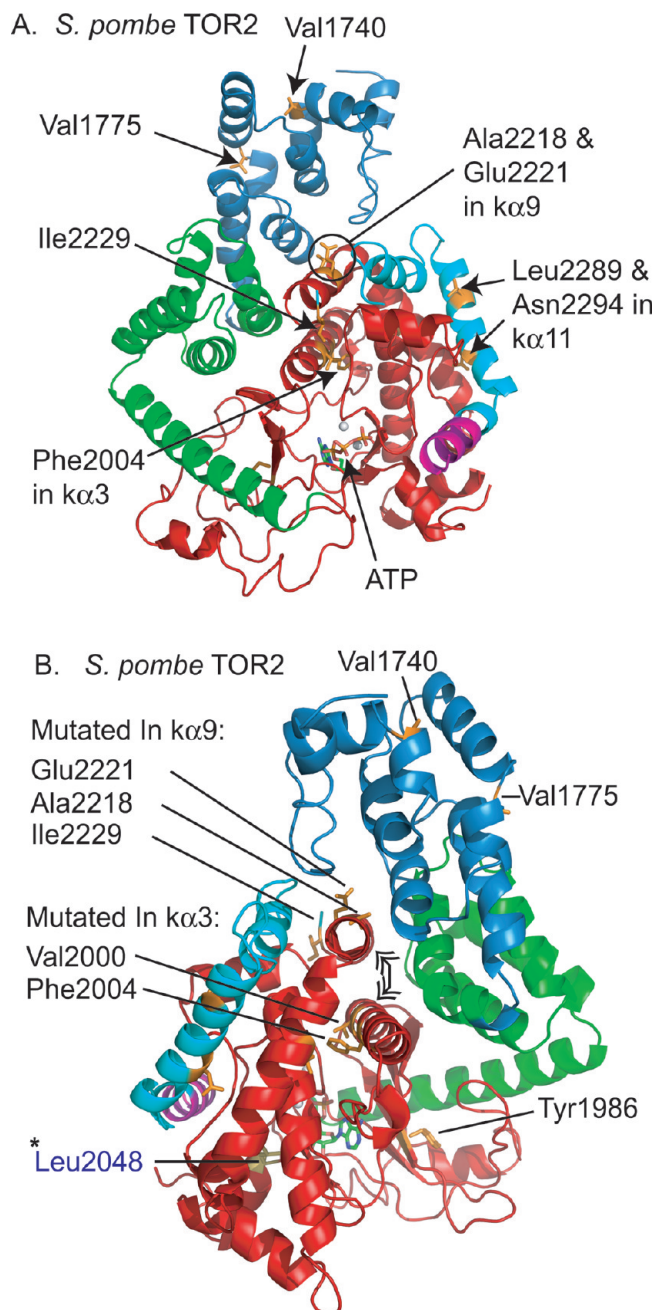
A. *S. pombe* TOR2

Val1740

Val1775

Ala2218 &
Glu2221
in kα9

Ile2229

Leu2289 &
Asn2294 in
kα11

Phe2004
in kα3

ATP

B. *S. pombe* TOR2

Val1740

Mutated In kα9:
Glu2221
Ala2218
Ile2229

Val1775

Mutated In kα3:
Val2000
Phe2004

Tyr1986

*Leu2048

Figure 6. Sites of activating mutations in *S. pombe* TOR2. A) Front and B) rear of molecule. Included in view is the site (L2048) of an inactivating mutation of *S. pombe* TOR2. Double arrow shows the key helices, kα3 (the RQD) and kα9 in PI3K-related kinases. Enlarge to see side chains (orange) of mutated residues.

W2176R mutation in TOR1 decreased affinity for caffeine. Trp2176 is conserved in all TORs and is in the ATP-binding pocket in our model (Figure 5). Trp2176 aligns with Ile881 in PI3KCγ and is in the short loop between kβ7 and kβ8. The view of Trp2176 (Figure 5, panel a) is from the back of the molecule, with the active site going into the page. The indole ring of Trp2176 is positioned close to the adenine ring of ATP (Figure 5, panel b). The conserved valines following these two residues are superimposed. The presence of tryptophan at this position in all TORs versus an aliphatic residue as in all PI3KCs is a significant difference in the adenine pockets.

Mutations of Ile1954 and Ala1957 in *S. cerevisiae* TOR1 increased TORC1 kinase activity, conferring caffeine resistance without affecting caffeine binding at the ATP site (*26*). The kinase activating mutations in TOR1 (I1954V, A1957V) are in the helical domain portion of the FRB domain in helix hA4 outside the catalytic domain (Figure 1). Similar activating mutations (I1957T, A1960V) in *S. cerevisiae* TOR2 confer mild resistance to the TORC1 inhibitor rapamycin (*29*), again suggesting that they indeed activate the kinase. Helix hA4 is between hB3 and hB4 in the helical domain of PI3KCγ.

In the fission yeast *S. pombe*, a selection for mutants that grow in the absence of the TOR activator Rhb1 (Rheb) produced 22 mutants with activating mutations in TOR2 (*30*). *S. Pombe* TOR2 (like *S. cerevisae* TOR1) is found predominantly in TORC1, and the biology of the TORs in the two yeasts is somewhat different as well (*31*). Interestingly, these activating TOR2 mutations also clustered in the helical domain and the kinase domain (Figure 6, panel A). Activating mutation Y1986C in *S. pombe* TOR2 is in kβ5 just before the RQD helix kα3; V2000L and F2004C are in the RQD helix (kα3); E2221K and A2218 are both in kα9. I2229T is just after the conserved DPL motif that ends kα9. L2289F and N2294I are in kα11.

The L2048S mutation in *S. pombe* TOR2 confers a cell cycle arrest and rapamycin hypersensitivity (*32*), suggesting that it is a loss-of-function mutation. This is consistent with the structural position of Leu2048 (Figure 6, panel B). Leu2048 is just after kβ8, following a threonine residue that is conserved in all TORs and PI3Ks. Importantly, Leu2048 is buried near kβ9 (the C-terminal anchor of the catalytic loop) and kβ10 (N-terminal anchor of DFG motif). The equivalent structurally important residue in PI3KCγ is Ile888.

Activating mutations in mammalian TOR were isolated in a chimeric TOR, *S. cerevisiae* TOR2 (1−1689) fused to rat TOR (1721−2549), by selecting in yeast the

ability to suppress a mutation in LST8 (a subunit of both TORC1 and TORC2) (*29*). Of the mutant strains that were generated by this selection, mutant SL1 had three mutations in the chimeric TOR, V2198A, L2216H, and L2260P. V2198A is in the RQD helix kα3 and, we suspect, causally related to the increased TOR activity, whereas L2216H and L2260P are in loops. Furthermore, L2260 is already a proline in *S. cerevisiae* TOR1 and TOR2. Mutant SL2 had two mutations, A2290V in the kα4−kα5 loop and K2440R in the FIT domain. Mutant SL3 had a single mutation, L2302Q, in kα5. SL1 had the most active TOR of the three mutant strains, supporting the importance of the RQD helix.

Finally, the *S. cerevisiae* TOR2 mutation G2129R causes caffeine sensitivity and reduces TOR2 activity (*33*). Gly2129 is adjacent to Lys2128, the essential, wortmannin-sensitive lysine conserved in TOR (Figure 3, panel b). This suggests that G2129R might inhibit kinase activity by positioning this lysine to interfere with ATP binding.

Structure-Based Design of TOR Inhibitors. (See Supplementary Figure S2 for chemical structures of all small molecules.) Apsel *et al.* (*5*) reported two pyrazolopyrimidine compounds that inhibit PI3KCα. Compound S1 is a precursor for PP242, reported as a selective inhibitor for TOR in both TORC1 and TORC2 (*18*). Compound S2, related to compound S1, was crystallized in human PI3KCγ (RCSB, PDB 3ene). Because the pyrazolopyrimidine rings of S1, S2, and PP242 are planar and quite similar, we asked if PP242 with its pyrazolopyrimidine ring can fit into PI3KCγ. We first placed S2 bound to human PI3KCγ (3ene) into the reference coordinates of our template porcine PI3KCγ (1e8x). The pyrazolopyrimidine of S2 with its attached methyl group fits neatly into PI3KC, with the second naphthalene ring positioned inside the pocket for adenine (Figure 7, panel A). The pyrazolopyrimidine of PP242 with its larger isopropyl moiety has clashes in PI3KCγ (Figure 7, panel B). In contrast, when we placed PP242 in TOR and superimposed the core pyrazolopyrimidine rings (*34*), TOR had sufficient space to accommodate the isopropyl moiety of the pyrazolopyrimidine ring of PP242 (Figure 7, panel C).

The dihedral angle for torsion between the two rings in S2 bound to PI3KCγ in 3ene was ∼45.4°, but in S2 the second ring is simple naphthalene. PP242 has a more polar 5-hydroxy indole moiety instead of naphthalene as its second ring (Supplementary Figure S2). The
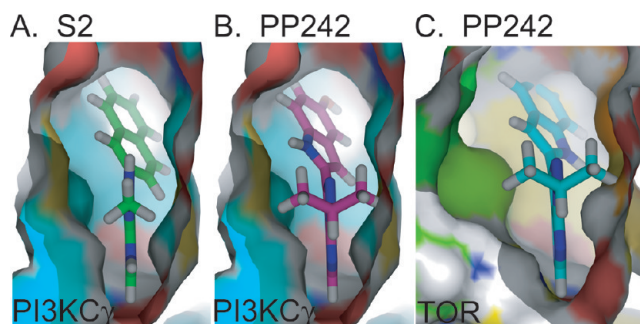

Figure 7. Manual docking of PP242 in TOR. A) S2 with its methyl group fit in PI3KCγ structure (3ene). B) PP242 hindered by wider isopropyl group in PI3KCγ. C) PP242 can fit into the TOR model. The pyrazolopyrimidine rings of PP242 and S2 were superimposed to position PP242 (see text). The images were generated with MacPyMol (DeLano Scientific).

potential for polar contacts for 5-hydroxy indole of PP242 in the adenine pocket was estimated in MacPymol by rotations about this bond maintaining the pyrazolopyrimidine portion fixed. PP242 with dihedral angles of −100° to −40° had potential for 3 polar contacts, with one in the adenine pocket. A dihedral angle of 130° is rotated 180 degrees and had potentially four polar contacts, with two in the adenine pocket.

We used AutoDock4 (*35, 36*) to predict a binding mode of PP242 to TOR (Figure 8, panel A), using compound S2 (Supplementary Figure S2) crystallized in human PI3KCγ (RCSB, PDB 3ene) to define a starting position. All of the residues shown have at least one atom within 4 Å of PP242. The 4-amino nitrogen of pyrazolopyrimidine makes a hydrogen bond to the backbone oxygen of Gly2238. Gly2238 is adjacent to the gatekeeper, near the hinge region. The 5-hydroxy of the indole of PP242 makes a polar contact with the ε-NH_2 of Lys2187 of TOR. Interestingly, the *m*-phenol of compound S1 (Supplementary Figure S2) interacts with the ε-NH_2 of Lys833 of human PI3KCγ (*5*). This helps explain PP242 inhibition. Lys2187 is required for catalysis. The 4-amine of the pyrazolopyrimidine is nearly positioned to make a π-cation bond with the aromatic ring of Tyr2225.

We also predicted a binding mode for NVP-BEZ235 to TOR using AutoDock4 (Figure 8, panel B). The coordinates for staurosporine in PI3KCγ (RCSB, PDB 1e8z) were used to generate a starting position for NVP-BEZ235 in TOR. Maira *et al.* (*16*) proposed a mode of binding of NVP-BEZ235 to PI3KCα based on this 1e8z
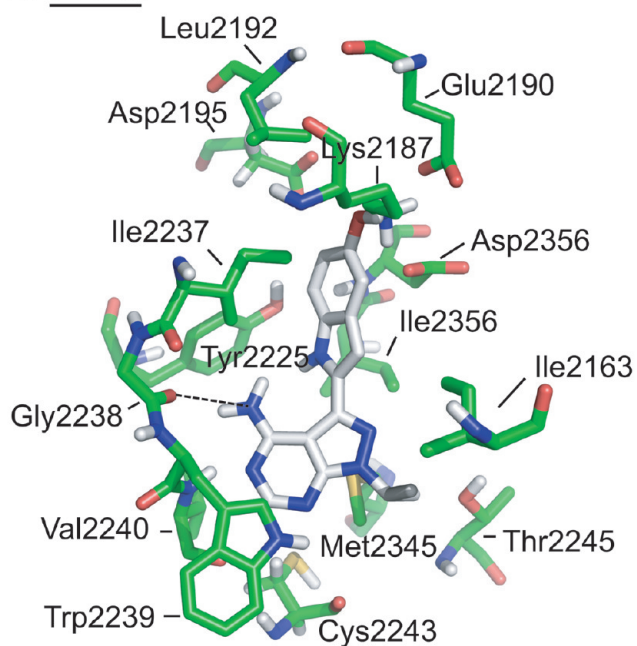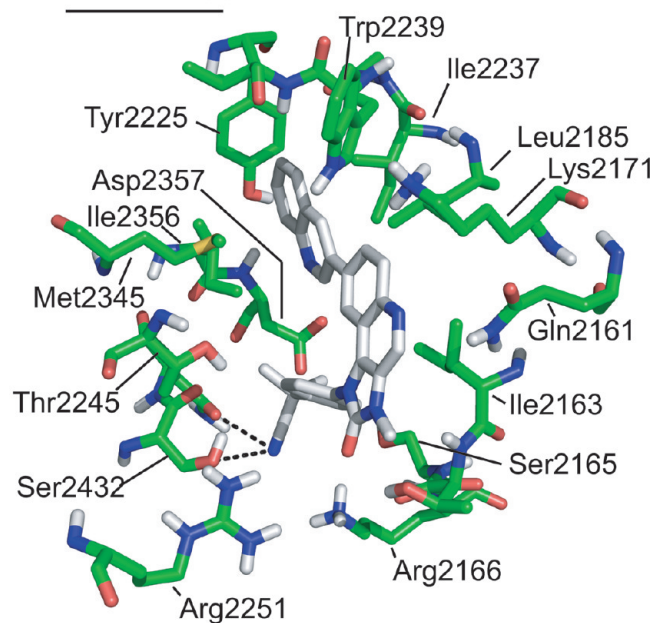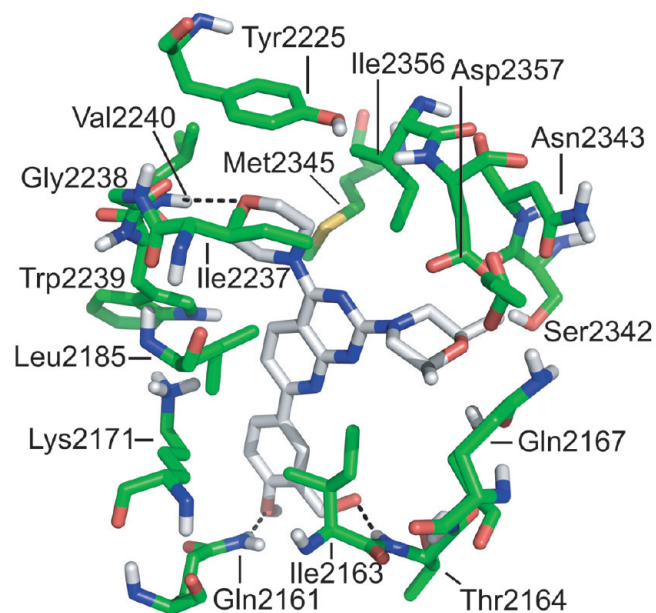
Figure 8. Optimized binding modes of lead compounds to the model of human TOR defined by AutoDock4 (Scripps). The TOR residues shown all have at least one atom within 4 Å of ligand. Ligands: carbon atoms, gray; nitrogen, blue; oxygen, red. Dashed lines, bonds. A) PP242. Leu2185 is omitted. B) NVP-BEZ235. C) Ku-0063794. Pro2169 and Lys2187 are omitted.

structure. The results we obtained for NVP-BEZ235 in the TOR model with AutoDock4 are somewhat different. The quinoline ring of NVP-BEZ235 is perpendicular to the aromatic ring of Tyr2225, taking a similar position as the adenine ring of ATP takes with the aromatic ring of the equivalent tyrosine in PI3KCγ. The nitrile nitrogen makes polar contacts in the catalytic loop with the Ser2342 side chain OH as well as with the Asn2343 backbone oxygen.

Ku-0063794 (Supplementary Figure S2) came from a chemical series identified in a drug discovery program for PIKK (ATM, ATR, DNA-activated PK) inhibitors, but had no prior report until a report of its specificity for TOR (*15*). Ku-0063794 is specific to TOR in TORC1 or TORC2 and does not inhibit PI3K (*15*). Ku-0063794 is an especially interesting small molecule. It has a central 1,3,8-triaza-napthalene core (also known chemically as pyrido[2,3-*d*]pyrimidine), and three radiating appendages, 4-[morpholine], 2-[dimethymorpholine], and 7-[3-hyroxymyethyl, 4-methoxy phenyl]. These appendages give the molecule an overall Y-shaped appearance.

We used ATP in PI3KCγ (1e8x) to approximate a starting position for Ku-0063794 for docking experiments with PI3KCγ and TOR. Ku-0063794 did not have any docked conformations to PI3KC, consistent with the specificity reported for TOR versus PI3KC. In the best of the docked conformations (Figure 8, panel C), Ku-0063794 binds with one arm of the Y in the adenine pocket and another along the hinge toward the position taken by the γ-phosphate of ATP. The morpholine ring oxygen was near Val2240. This potential interaction is of interest because the PI3K inhibitor LY22490 binds to PI3KCγ in a mode wherein oxygen of the morpholine ring is hydrogen bonded to backbone nitrogen of Val882 of PI3KCγ. Val2240 of TOR is the equivalent residue.

The OH of the 3-hydroxymethyl is hydrogen bonded to the side chain of Gln2161. The OH of the 4-methoxy is hydrogen bonded to the backbone nitrogen of Thr2164. Conformations rotated ∼180 around the bond connecting the base of the Y to the core were 1.5 kCal less favored but still plausible, and placed the dimethylmorpholine ring in the adenine pocket near Ty2225, Ile2356, Ile2237, and Leu23185. In this pose, Ku-0063794 retains the H-bonding interactions with Gln2161 and Thr2164.

A shortcoming of the docking studies is that the predicted negative energies of binding do not account for the reported nanomolar K_i for TOR inhibition in cells by
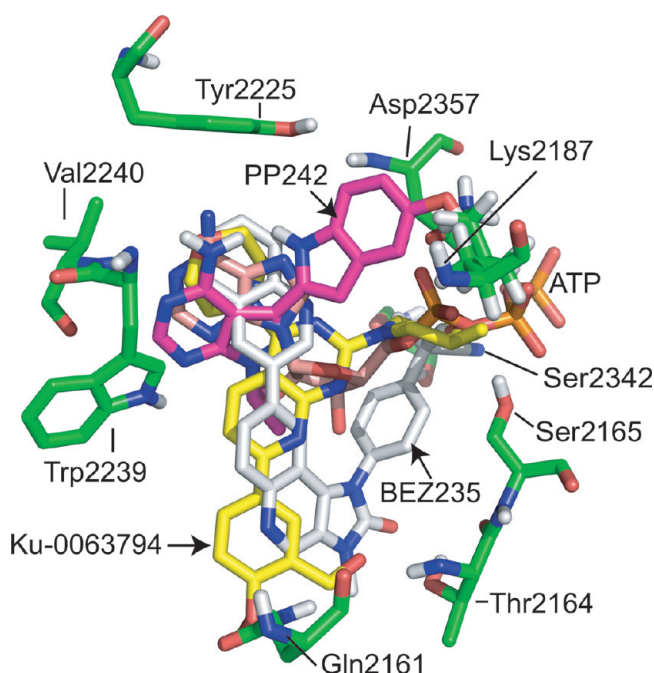

Figure 9. Superposition of the predicted binding modes of PP242, NVP-BEZ235, and Ku-0063794. PP242, carbons, magenta; NVP-BEZ235, carbons, gray; Ku-0063794, carbons, yellow.

PP242 (*18*), NVP-BEZ235 (*16*), and Ku-0063794 (*15*). The highest scoring conformations with AutoDock4 gave us −7.08 kCal/mol, −8.82 kCal/mol, and −8.44 kCal/mol for PP242, NVP-BEZ235, and Ku-0063794, respectively. This may be due to an imperfect model or to AutoDock4 scoring. Both, especially the former possibility, are likely. Work to refine the model is ongoing. AutoDock4 is not always accurate for small molecule inhibitors in pockets where hydrophobic interactions and hydrogen bonds are very important (*37*).

Achieving TOR Specificity by Use of a Novel Pharmacophore Space. A novel space for pharmacophores exists in a channel that runs from the bottom surface of TOR inward toward the ATP and substrate pockets. PI3KC has, and TOR is predicted to have, a relatively flat bottom (Figure 4 and Supplementary Figure S1). The longitudinal axis of ATP is roughly perpendicular to the axis of this channel. A pocket that lies immediately adjacent to the γ-phosphate may serve to position substrate OH for phosphate transfer.

The predicted binding modes of PP242, NVP-BEZ235, and Ku-0063794 are compared to ATP in Figure 9. All three compounds have a ring roughly perpendicular to

A. Use of the novel pharmacophore space by PP242

PP242

B. Use of the novel pharmacophore space by NVP-BEZ235

NVP-BEZ235

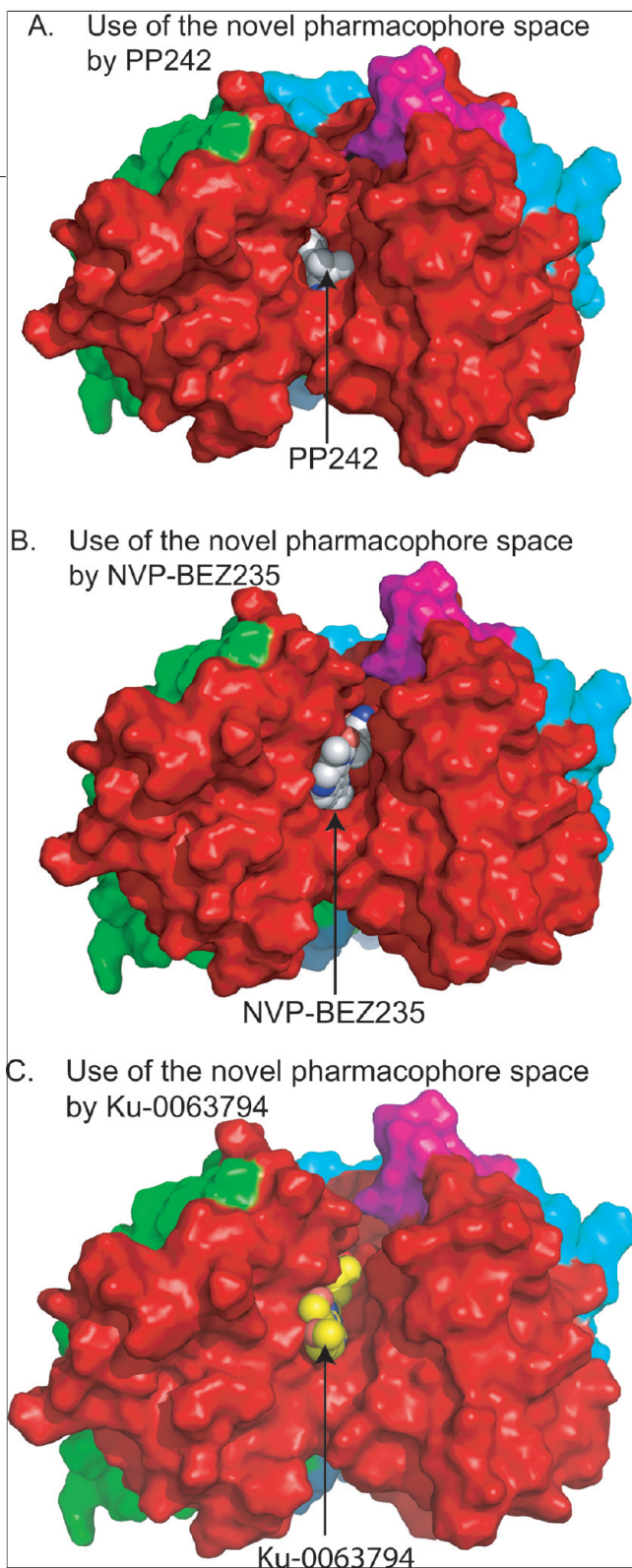**C. Use of the novel pharmacophore space by Ku-0063794**

Ku-0063794

Figure 10. Differences in use of a novel pharmacophore space may be responsible for TOR specificity of Ku-0063794. Surface view of TOR generated by MacPymol (Delano Scientific), viewed roughly perpendicular to the space, the surface termed "bottom". TOR domains are colored as before. A) Docked PP242. B) Docked NVP-BEZ235. C) Docked Ku-0063794. Note how TOR-specific Ku-0063794 packs into and nearly fills this space.

Tyr2225 similar to ATP. Ku-0063794 is TOR-specific and PP242 is TOR-selective, while BEZ-235 inhibits both TOR and PI3KC. Their specificity may be rationalized by the way these lead compounds make use of the novel pharmacophore space in TOR. The isopropyl group of PP242 is too wide to be accommodated at a critical position in the channel in PI3KCγ (Figure 7), yet overall PP242 is the smallest compound and occupies the smallest portion of the pharmacophore space. NVP-BEZ235 and Ku-0063794 make different use of the pharmacophore space. A portion of NVP-BEZ235 projects into the space, but its 4′-(2-cyano-2-propyl) phenyl group is hooked back by its geometry so that the nitrile is placed near residues in the catalytic loop. Ku-0063794 is sufficiently long in the portion we call the base of the Y to bring the base's polar groups into contact with polar surface residues that line the opening of the channel upon the bottom surface. Ku-0063794 must be too large for the smaller space in PI3KC, as Ku-0063794 had no docked conformations in PI3KC. The dual specificity of BEZ235 for TOR and PI3KC may be due to its unusual geometry that keeps major parts of it in the conserved ATP binding pockets of the two kinases. The differences in degree of occupancy of the novel pharmacophore space in TOR can be appreciated by comparing surface views of docked PP242, NVP-BEZ235, and Ku-0063794 (Figure 10).

DISCUSSION

We discovered that activating mutations in TOR identified in genetic selections are in the helical, catalytic, and FIT domains in our structure for TOR. Oncogenic mutations in PI3KCα are also concentrated in the helical and catalytic domains and in the C-terminus in helix kα11 that corresponds to a portion of the FIT domain. In the catalytic domain of PI3KCα, oncogenic mutations were found at Cys901 and Phe909 in kα6, at Ser1008 in kα9, at Thr1025 in kα10, and at Met1043 and His1047 in kα11 (Figure 1). Activating mutations in the catalytic region of *S. pombe* TOR2 were found in or near kα3, kα5, kα9, and kα11 (*30*). Activating mutations in human TOR were found in kα3, the kα4−kα5 loop and the FIT domain (mutant SL2), and kα5. The overlap of locations of activating TOR mutations and locations of oncogenic mutations in PI3KCα supports structural similarity between TOR and PI3KC.

In the helical domain of PI3KCα, oncogenic mutations cluster in residues Glu542, Glu545, Gln546, and

Gln661 (*38*). In the structural alignment (Figure 1; also see ref 6), this hotspot is near hB1 of PI3KCγ. In the determined structures for PI3KCα (RCSB, PDB 2d0, 3hhm, 3hiz), these residues make contact with the niSH2 fragment of the p85 adapter (*4, 39*).

In the catalytic region of PI3KCα, oncogenic mutations cluster in residues Met1043 and His1047 in kα11 and at Gly1049 in the short loop between kα11 and kα12 (Figure 1) (*38*). Mutations at His1047 are more frequent, and their oncogenic effects are potent (*40*). Helix kα11 in PI3KCγ corresponds to helix αk12 in PI3KCα (*4, 39*), the last helix identified by crystallography at the C-terminus in PI3KCα.

The two activating mutations L2289F and N2294I in *S. pombe* TOR2 are in kα11. These are a just a few residues from the His1047 oncogenic hotspot in PI3KCα. His1047 was aligned to Gly2510 in human TOR (Figure 1). Between Asp2506 and Gly2510, we discovered a KLT motif that is conserved in the ~100 TORs and found in the FIT domain of ATM (manuscript in preparation). Tip60 acetylates Lys3016 in the KLT motif of ATM, and Lys3016 is required for ATM function (*41*).

Allosteric regulation of ATR requires the FIT domain of ATR (*42, 43*). Protein TopBP1 (topoisomerase (DNA) II binding protein 1) binds PRD (PIKK regulatory domain) (*43*) and activates an ATR: ATRIP (ATR interacting protein) complex. Scanning mutagenesis of the PRD (equivalent in definition to FIT domain) identified mutations (K2589E and HVL2591AAA) that did not inhibit the basal kinase of ATR but inhibited its activation by TopBP1 (*43*). TopBP1 increased kinase activity *in vitro*, chiefly by decreasing the Km for substrate (*42*). Where are the equivalent residues in TOR? ATR Lys2589 aligns to the short loop between kα10 and kα11, and residues His2591, Val2592, and Leu2593 align to kα11 (data not shown). This observation indicates a likelihood that kα11 helix is important in regulation of all PIKKs and PI3KCs, by multiple mechanisms.

Two hypotheses emerged in building a model of TOR. The first hypothesis is that the helical domain (FAT plus FRB) of TOR may have a similar general relation in space to its catalytic domain as the helical domain of PI3K has to its catalytic domain, also suggested in ref 47. Our model cannot predict this portion accurately on the basis of homology because the sequence similarity is minimal. The second hypothesis is that the C-terminus of TOR contains a variable insertion (in vertebrates, including the conserved motif with the S2481 and S2484 phosphorylation sites) that may lie on a surface where a much shorter surface loop lies on the surface of PI3K near the active site. This insertion is in a segment of TOR we name the FIT domain for future discussion. The FIT domain also contains helices (kα10−12) that correspond to conserved helices at the C-terminus of PI3KCs, to which is appended or incorporated the FATC domain not present in PI3K.

Recently, the ATP-binding site of TOR was modeled to a PI3KCγ structure to rationalize the structure−activity relationship of the novel TOR-selective inhibitor 6-(1*H*-indol-5-yl)-4-morpholin-4-yl-1-[1-(pyridin-3-ylmethyl)piperidin-4-yl]-1*H*-pyrazolo[3,4-*d*]pyrimidine (also referred to as 5u) (*44*). Few details of the model are provided, but having a model facilitated optimization of a lead compound. Template PI3KCγ contained a co-crystallized 4-[morpholin-4yl] pyrazolopyrimidine, and interestingly OH of the morpholine contacts Val882 in the adenine pocket of PI3KCγ. The molecular core of 4-[morpholine-4yl] pyrazolopyrimidine is more similar to the core of 4-[morpholine] pyrido[2,3-*d*]pyrimidine in small molecule Ku-0063794 than to the pyrazolopyrimidine of PP242 (see Supplementary Figure S2) because of this morpholine moiety. In the putative binding mode for 5u to the ATP site in TOR, the morpholine makes a hydrogen bond to the equivalent residue, Val2240, as we predict for the morpholine moiety in Ku-0063794. Of more interest, the NH_2 of 6-[indole] moiety of 5u is predicted to contact the COOH of Asp2195 in the RQD motif of kα3, the precise element that we hypothesize is important for kinase activity of PI3KC and PIKKs.

METHODS

Informatics. We obtained sequences for TORs from NCBI, www.ensembl.org, and the Broad Institute. We compared sequences using ClustalW (Gibson) using the server at Pole-Bioinformatique-Lyonnais. The sequences were inspected and trimmed to commence at ~1800 by BLAST to human TOR1864−2549. These were compared to large subsets of PI3K (classes I−III) and to each other to deduce what was conserved in PI3KC or TOR.

Structural Alignment. TORs (human, mouse, *S. cerevisiae* (TOR1, TOR2) and *S. pombe* TOR2) were aligned manually, in a slow process, with sequences for human and zebrafish PI3KCα and human and pig PI3KCγ. Ability to view sequences with color codings, including for predicted α-helix, β-sheet, and structural

position, and other comparative modes in MacVector was invaluable. Cn3D at the NCBI structure depository was helpful in viewing structural elements and especially the structural position (interior versus surface) of loops.

SwissModel Server. Manual alignments of human and yeast TORs to template were exported in FASTA format to the Swiss-Model server (*25*). We used a MacBook Pro (OS10.5.7 and Xtools) with DeepView v4.0 (Swiss Institute of Bioinformatics), PyMol (DeLano Scientific), Chimera (UCSF), and the MGL 1.6.0 package of programs from Scripps Research Institute (*35, 36*). Magic Fit in DeepView was used for superposition of chains to place structure 3ene in the 1e8x reference. For docking, models for human and yeast TOR with stubs replacing missing loops were first analyzed by Molprobity to add all hydrogens and to flip Asn, Gln, and His bonds (*45*). The reduced model with flips was minimized for energy in Chimera, and Chimera was used to convert formats. (The PRODRG2 server (*46*) was used to produce small molecule structures for AutoDock4 for small molecules PP242 (*5*) NVP-BEZ235 (*16*) and Ku-0063794 (*15*).

MacPyMOL was used for production of most figures and for preset analyses of ligand sites (*34*) .

Docking Analyses. MGL tools 1.6.0 with AutoGrid4 and AutoDock4 (Scripps) were used for docking studies. Most were with 256 runs with 2,500,000 energy evaluations with the Lamarckian algorithm for generating populations of 150 random positions from the starting position (see text) and otherwise default settings (*35*).

REFERENCES

1. Brachmann, S., Fritsch, C., Maira, S. M., and Garcia-Echeverria, C. (2009) PI3K and mTOR inhibitors: a new generation of targeted anticancer agents, *Curr. Opin. Cell Biol. 21*, 194–198.
2. Wullschleger, S., Loewith, R., and Hall, M. N. (2006) TOR signaling in growth and metabolism, *Cell 124*, 471–484.
3. Guertin, D. A., and Sabatini, D. M. (2007) Defining the role of mTOR in cancer, *Cancer Cell 12*, 9–22.
4. Huang, C. H., Mandelker, D., Schmidt-Kittler, O., Samuels, Y., Velculescu, V. E., Kinzler, K. W., Vogelstein, B., Gabelli, S. B., and Amzel, L. M. (2007) The structure of a human p110alpha/p85alpha complex elucidates the effects of oncogenic PI3Kalpha mutations, *Science (New York, N.Y.) 318*, 1744–1748.
5. Apsel, B., Blair, J. A., Gonzalez, B., Nazif, T. M., Feldman, M. E., Aizenstein, B., Hoffman, R., Williams, R. L., Shokat, K. M., and Knight, Z. A. (2008) Targeted polypharmacology: discovery of dual inhibitors of tyrosine and phosphoinositide kinases, *Nat. Chem. Biol. 4*, 691–699.
6. Walker, E. H., Perisic, O., Ried, C., Stephens, L., and Williams, R. L. (1999) Structural insights into phosphoinositide 3-kinase catalysis and signalling, *Nature 402*, 313–320.
7. Walker, E. H., Pacold, M. E., Perisic, O., Stephens, L., Hawkins, P. T., Wymann, M. P., and Williams, R. L. (2000) Structural determinants of phosphoinositide 3-kinase inhibition by wortmannin, LY294002, quercetin, myricetin, and staurosporine, *Mol. Cell 6*, 909–919.
8. Abbreviations and acronyms: TOR, target of rapamycin (gene ID 56718); TOR domains: (i) FAT, named for FRAP, ATM and TRRAP (pfam00259), (ii) FRB, named for FKBP12:Rapamycin Binding (pfam08771); FIT, Found in TOR (residues 2427−2516), this manuscript; FATC, named for FRAP, ATM, TRRAP C-terminal (pfam02260).
9. Marone, R., Cmiljanovic, V., Giese, B., and Wymann, M. P. (2008) Targeting phosphoinositide 3-kinase: moving towards therapy, *Biochim. Biophys. Acta 1784*, 159–185.
10. Pacold, M. E., Suire, S., Perisic, O., Lara-Gonzalez, S., Davis, C. T., Walker, E. H., Hawkins, P. T., Stephens, L., Eccleston, J. F., and Williams, R. L. (2000) Crystal structure and functional analysis of Ras binding to its effector phosphoinositide 3-kinase gamma, *Cell 103*, 931–943.
11. Abraham, R. T. (2004) PI 3-kinase related kinases: 'big' players in stress-induced signaling pathways, *DNA Repair 3*, 883–887.
12. Vander Heiden, M. G., Cantley, L. C., and Thompson, C. B. (2009) Understanding the Warburg effect: the metabolic requirements of cell proliferation, *Science (New York, N.Y.) 324*, 1029–1033.
13. Carracedo, A., Ma, L., Teruya-Feldstein, J., Rojo, F., Salmena, L., Alimonti, A., Egia, A., Sasaki, A. T., Thomas, G., Kozma, S. C., Papa, A., Nardella, C., Cantley, L. C., Baselga, J., and Pandolfi, P. P. (2008) Inhibition of mTORC1 leads to MAPK pathway activation through a PI3K-dependent feedback loop in human cancer, *J. Clin. Invest. 118*, 3065–3074.
14. Fan, Q. W., Knight, Z. A., Goldenberg, D. D., Yu, W., Mostov, K. E., Stokoe, D., Shokat, K. M., and Weiss, W. A. (2006) A dual PI3 kinase/mTOR inhibitor reveals emergent efficacy in glioma, *Cancer Cell 9*, 341–349.
15. Garcia-Martinez, J. M., Moran, J., Clarke, R. G., Gray, A., Cosulich, S. C., Chresta, C. M., and Alessi, D. R. (2009) Ku-0063794 is a specific inhibitor of the mammalian target of rapamycin (mTOR), *Biochem. J. 421*, 29–42.
16. Maira, S. M., Stauffer, F., Brueggen, J., Furet, P., Schnell, C., Fritsch, C., Brachmann, S., Chene, P., De Pover, A., Schoemaker, K., Fabbro, D., Gabriel, D., Simonen, M., Murphy, L., Finan, P., Sellers, W., and Garcia-Echeverria, C. (2008) Identification and characterization of NVP-BEZ235, a new orally available dual phosphatidylinositol 3-kinase/mammalian target of rapamycin inhibitor with potent *in vivo* antitumor activity, *Mol. Cancer Ther. 7*, 1851–1863.
17. Thoreen, C. C., Kang, S. A., Chang, J. W., Liu, Q., Zhang, J., Gao, Y., Reichling, L. J., Sim, T., Sabatini, D. M., and Gray, N. S. (2009) An ATP-competitive mammalian target of rapamycin inhibitor reveals rapamycin-resistant functions of mTORC1, *J. Biol. Chem. 284*, 8023–8032.
18. Feldman, M. E., Apsel, B., Uotila, A., Loewith, R., Knight, Z. A., Ruggero, D., and Shokat, K. M. (2009) Active-site inhibitors of mTOR target rapamycin-resistant outputs of mTORC1 and mTORC2, *PLoS Biol. 7*, e38.
19. Johnson, D. A., Akamine, P., Radzio-Andzelm, E., Madhusudan, M., and Taylor, S. S. (2001) Dynamics of cAMP-dependent protein kinase, *Chem. Rev. 101*, 2243–2270.
20. Holz, M. K., and Blenis, J. (2005) Identification of S6 kinase 1 as a novel mammalian target of rapamycin (mTOR)-phosphorylating kinase, *J. Biol. Chem. 280*, 26089–26093.
21. Edinger, A. L., and Thompson, C. B. (2004) An activated mTOR mutant supports growth factor-independent, nutrient-dependent cell survival, *Oncogene 23*, 5654–5663.
22. Copp, J., Manning, G., and Hunter, T. (2009) TORC-specific phosphorylation of mammalian target of rapamycin (mTOR): phospho-Ser2481 is a marker for intact mTOR signaling complex 2, *Cancer Res. 69*, 1821–1827.

23. Peterson, R. T., Beal, P. A., Comb, M. J., and Schreiber, S. L. (2000) FKBP12-rapamycin-associated protein (FRAP) autophosphorylates at serine 2481 under translationally repressive conditions, *J. Biol. Chem. 275*, 7416–7423.

24. Dames, S. A., Mulet, J. M., Rathgeb-Szabo, K., Hall, M. N., and Grzesiek, S. (2005) The solution structure of the FATC domain of the protein kinase target of rapamycin suggests a role for redox-dependent structural and cellular stability, *J. Biol. Chem. 280*, 20558–20564.

25. Bordoli, L, Kiefer, F., Arnold, K., Benkert, P., Battey, J., and Schwede, T. (2009) Protein structure homology modeling using SWISS-MODEL workspace, *Nat. Protoc. 4*, 1–13.

26. Reinke, A., Chen, J. C., Aronova, S., and Powers, T. (2006) Caffeine targets TOR complex I and provides evidence for a regulatory link between the FRB and kinase domains of Tor1p, *J. Biol. Chem. 281*, 31616–31626.

27. Blasina, A., Price, B. D., Turenne, G. A., and McGowan, C. H. (1999) Caffeine inhibits the checkpoint kinase ATM, *Curr. Biol. 9*, 1135–1138.

28. Wanke, V., Cameroni, E., Uotila, A., Piccolis, M., Urban, J., Loewith, R., and De Virgilio, C. (2008) Caffeine extends yeast lifespan by targeting TORC1, *Mol. Microbiol. 69*, 277–285.

29. Ohne, Y., Takahara, T., Hatakeyama, R., Matsuzaki, T., Noda, M., Mizushima, N., and Maeda, T. (2008) Isolation of hyperactive mutants of mammalian target of rapamycin, *J. Biol. Chem. 283*, 31861–31870.

30. Urano, J., Sato, T., Matsuo, T., Otsubo, Y., Yamamoto, M., and Tamanoi, F. (2007) Point mutations in TOR confer Rheb-independent growth in fission yeast and nutrient-independent mammalian TOR signaling in mammalian cells, *Proc. Natl. Acad. Sci. U.S.A. 104*, 3514–3519.

31. Sturgill, T. W., and Hall, M. N. (2007) Holding back TOR advances mitosis, *Nat. Cell Biol. 9*, 1221–1222.

32. Hayashi, T., Hatanaka, M., Nagao, K., Nakaseko, Y., Kanoh, J., Kokubu, A., Ebe, M., and Yanagida, M. (2007) Rapamycin sensitivity of the Schizosaccharomyces pombe tor2 mutant and organization of two highly phosphorylated TOR complexes by specific and common subunits, *Genes Cells 12*, 1357–1370.

33. deHart, A. K., Schnell, J. D., Allen, D. A., Tsai, J. Y., and Hicke, L. (2003) Receptor internalization in yeast requires the Tor2-Rho1 signaling pathway, *Mol. Biol. Cell 14*, 4676–4684.

34. Delano, W. (2009) The PyMOL Molecular Graphics System 1.01; www.pymol.sourceforge.net.

35. Morris, G. M., Huey, R., Lindstrom, W., Sanner, M. F., Belew, R. K., Goodsell, D. S., and Olson, A. J. (2009) AutoDock4 and AutoDockTools4: Automated docking with selective receptor flexibility, *J. Comput. Chem. 30*, 2785–2791.

36. Morris, G. M., Huey, R., Olson, A. J. (2008) Using AutoDock for ligand-receptor docking, *Curr. Protoc. Bioinf.* Chapter 8, Unit 8.14.

37. Buzko, O. V., Bishop, A. C., and Shokat, K. M. (2002) Modified AutoDock for accurate docking of protein kinase inhibitors, *J. Comput.-Aided Mol. Des. 16*, 113–127.

38. Samuels, Y., Wang, Z., Bardelli, A., Silliman, N., Ptak, J., Szabo, S., Yan, H., Gazdar, A., Powell, S. M., Riggins, G. J., Willson, J. K., Markowitz, S., Kinzler, K. W., Vogelstein, B., and Velculescu, V. E. (2004) High frequency of mutations of the PIK3CA gene in human cancers, *Science (New York, N.Y.) 304*, 554.

39. Mandelker, D., Gabelli, S. B., Schmidt-Kittler, O., Zhu, J., Cheong, I., Huang, C. H., Kinzler, K. W., Vogelstein, B., and Amzel, L. M. (2009) A frequent kinase domain mutation that changes the interaction between PI3Kalpha and the membrane, *Proc. Natl. Acad. Sci. U.S.A. 106*, 16996–17001.

40. Samuels, Y., Diaz, L. A., Jr., Schmidt-Kittler, O., Cummins, J. M., Delong, L., Cheong, I., Rago, C., Huso, D. L., Lengauer, C., Kinzler, K. W., Vogelstein, B., and Velculescu, V. E. (2005) Mutant PIK3CA promotes cell growth and invasion of human cancer cells, *Cancer Cell 7*, 561–573.

41. Sun, Y., Xu, Y., Roy, K., and Price, B. D. (2007) DNA damage-induced acetylation of lysine 3016 of ATM activates ATM kinase activity, *Mol. Cell. Biol. 27*, 8502–8509.

42. Mordes, D. A., and Cortez, D. (2008) Activation of ATR and related PIKKs, *Cell Cycle 7*, 2809–2812.

43. Mordes, D. A., Glick, G. G., Zhao, R., and Cortez, D. (2008) TopBP1 activates ATR through ATRIP and a PIKK regulatory domain, *Genes Dev. 22*, 1478–1489.

44. Nowak, P., Cole, D. C., Brooijmans, N., Bursavich, M. G., Curran, K. J., Ellingboe, J. W., Gibbons, J. J., Hollander, I., Hu, Y. B., Kaplan, J., Malwitz, D. J., Toral-Barza, L., Verheijen, J., Zask, A., Zhang, W. G., Yu, K. (2009) Discovery of potent and selective inhibitors of the mammalian target of rapamycin (mTOR) kinase. *J. Med. Chem.* Published ASAP October 19, 2009; DOI: 10.1021/jm9012642.

45. Davis, I. W., Leaver-Fay, A., Chen, V. B., Block, J. N., Kapral, G. J., Wang, X., Murray, L. W., Arendall, W. B., 3rd, Snoeyink, J., Richardson, J. S., and Richardson, D. C. (2007) MolProbity: all-atom contacts and structure validation for proteins and nucleic acids, *Nucleic Acids Res. 35*, W375—383.

46. Schuttelkopf, A. W., and van Aalten, D. M. (2004) PRODRG: a tool for high-throughput crystallography of protein-ligand complexes, *Acta Crystallogr. Sect. D: Biol. Crystallogr. 60*, 1355–1363.

47. Lempiainen, H., and Halazonetis, T. D. (2009) Emerging common themes in regulation of PIKKs and PI3Ks, *EMBO J.* **2009** *28*, 3067–3073.